

Original Research

The Ability of Clinically Relevant Chemotherapeutics to Induce Immunogenic Cell Death in Squamous Cell Carcinoma

Zhenjie He^{1,†}, Xinming Jing^{1,†}, Xiaoyan Dai¹, Lingbo Bao^{1,2}, Xiao Yang¹, Yanli Xiong^{1,*}, Mengxia Li^{1,*}¹Cancer Center of Daping Hospital, Third Military Medical University, 400038 Chongqing, China²Department of Oncology, General Hospital of Western Theatre Command, 610000 Chengdu, Sichuan, China*Correspondence: xiongyli@outlook.com (Yanli Xiong); mengxia.li@outlook.com (Mengxia Li)

†These authors contributed equally.

Academic Editor: Roberto Bei

Submitted: 16 January 2024 Revised: 23 February 2024 Accepted: 15 March 2024 Published: 22 April 2024

Abstract

Background: Immunogenic cell death (ICD) is a crucial mechanism for triggering the adaptive immune response in cancer patients. Damage-associated molecular patterns (DAMPs) are critical factors in the detection of ICD. Chemotherapeutic drugs can cause ICD and the release of DAMPs. The aim of this study was to assess the potential for paclitaxel and platinum-based chemotherapy regimens to induce ICD in squamous cell carcinoma (SCC) cell lines. In addition, we examined the immunostimulatory effects of clinically relevant chemotherapeutic regimens utilized in the treatment of SCC. **Methods:** We screened for differentially expressed ICD markers in the supernatants of three SCC cell lines following treatment with various chemotherapeutic agents. The ICD markers included Adenosine Triphosphate (ATP), Calreticulin (CRT), Annexin A1 (ANXA 1), High Mobility Group Protein B1 (HMGB1), and Heat Shock Protein 70 (HSP70). A vaccination assay was also employed in C57BL/6J mice to validate our *in vitro* findings. Lastly, the levels of CRT and HMGB1 were evaluated in Serum samples from SCC patients. **Results:** Addition of the chemotherapy drugs cisplatin (DDP), carboplatin (CBP), nedaplatin (NDP), oxaliplatin (OXA) and docetaxel (DOC) increased the release of ICD markers in two of the SCC cell lines. Furthermore, mice that received vaccinations with cervical cancer cells treated with DDP, CBP, NDP, OXA, or DOC remained tumor-free. Although CBP induced the release of ICD-associated molecules *in vitro*, it did not prevent tumor growth at the vaccination site in 40% of mice. In addition, both *in vitro* and *in vivo* results showed that paclitaxel (TAX) and LBP did not induce ICD in SCC cells. **Conclusion:** The present findings suggest that chemotherapeutic agents can induce an adjuvant effect leading to the extracellular release of DAMPs. Of the agents tested here, DDP, CBP, NDP, OXA and DOC had the ability to act as inducers of ICD.

Keywords: squamous carcinoma; chemotherapy; immunogenic cell death; damage-associated molecular pattern

1. Introduction

Tumor cell death is the ultimate biological and therapeutic objective of antitumor therapy [1]. Recently, immunotherapy has become established as a new milestone in cancer treatment. However, clinical trials indicate that only 10–30% of patients derive therapeutic benefit from immune checkpoint inhibitors (ICIs) due to suboptimal responses [2]. The crucial role of the physiological process induced by cell death in determining the therapeutic efficacy of ICIs is often overlooked [3–5]. During the development and homeostasis of the vertebrate immune system, cells develop a highly orchestrated mode of immunologically silent, or tolerogenic, cell death. These dead/dying cells promote innate and adaptive immune responses without inducing inflammation. Immunogenic cell death (ICD) is a type of cell death that kills tumor cells by stimulating and directing the adaptive immune response against them. ICD depends on endoplasmic reticulum stress and the secretion of damage-associated molecular patterns (DAMPs) by dying tumor cells [6]. Cells that undergo ICD in the presence of anticancer therapeutics undergo regulated cell

death that initiates adaptive immune responses associated with immune memory. Consequently, drugs that are capable of inducing ICD are considered to be clinically significant because of their ability to enhance therapeutic efficacy by recruiting antitumoral immunity.

The canonical DAMPs include calreticulin (CRT), high mobility group protein 1 (HMGB1), adenosine triphosphate (ATP), membrane-connected protein A1 (ANXA1), and heat-shock protein 70 (HSP70) [7]. These ectopically expressed DAMPs may represent a promising approach for activating the tumor immune microenvironment, thereby improving the sensitivity of immunotherapy [8]. Consistent with this notion, it has been reported that drug-induced ICD is positively associated with the therapeutic response and enhances antitumor CD8⁺ T-cell immunity in the clinical setting. There is accumulating clinical evidence that several inducers of ICD commonly used in the treatment of cancer patients can synergize with immunotherapy involving ICIs [9,10]. However, only a few anticancer agents are acknowledged to be bona fide inducers of ICD, including oxaliplatin (OXA),



cyclophosphamide (CPA), mitoxantrone, epirubicin, and doxorubicin. Most conventional chemotherapies do not induce ICD when used as monotherapy, including cisplatin (DDP) and gemcitabine [11,12].

The aim of this study was therefore to generate comprehensive data on the ability of clinically relevant chemotherapeutic agents to induce ICD in squamous cell carcinoma (SCC). To do this, we compared the immunogenicity of different chemotherapeutics in specific cancer models. We employed an *in vivo* vaccination assay, considered as the “gold standard”, using a panel of human and murine cervical SCC cell lines. This was used to evaluate the ability of different therapeutic agents to induce ICD [13]. We also investigated the immunoadjuvant role of signature DAMPs in promoting anti-tumor immune responses. The percentage of tumor-free mice is an indicator of the immunogenicity of the tested compounds. Consequently, these *in vitro* and *in vivo* experiments provided novel insights into the potential of various first- and second-line chemotherapeutic agents for the treatment of cervical SCC.

2. Materials and Methods

2.1 Cell Lines and Cell Culture

Eca109 (RRID: CVCL 6898), Siha (RRID: CVCL 0032) and U14 (RRID: CVCL 9U56), cancer cells were purchased from the Cell Bank of Chinese Academy of Sciences (Shanghai, China) and authenticated by the supplier (Shanghai, China). Siha and U14 cultured in Dulbecco’s modified eagle medium (DMEM) (Pricella; PM150210, Wuhan, China), and Eca109 were cultured in the RPMI1640 (Pricella; PM150110, Wuhan, China) medium, supplemented with 10% fetal bovine Serum (Cytiva; SH30401.01, Attleboro, MA, USA) and 1% penicillin–streptomycin (Cytiva; SV30010, Attleboro, MA, USA). All cell lines were validated by STR profiling and tested negative for mycoplasma. Cells were all cultured in a humidified incubator at 37 °C and 5% CO₂.

2.2 Cytotoxicity of Different Chemotherapies

The following chemotherapeutic agents were used: cisplatin (DDP), carboplatin (CBP), nedaplatin (NDP), lobaplatin (LBP), OXA, paclitaxel (TAX), docetaxel (DOC). All medications donated from the Pharmaceutical Dispensing Center of the Army Medical Center except for the OXA (Selleck; S1224, Houston, TX, USA) and DOC (Selleck; S1148, Houston, TX, USA). To evaluate cytotoxicity of the different chemotherapeutic agents, Eca109, Siha, and U14 cells were seeded in 96-well plates (NEST; 701002, Shanghai, China), incubated overnight. Eca109 cells treated for 48 h with either DDP (0–16 μM), CBP (0–512 μM), NDP (0–128 μM), LBP (0–512 μM), OXA (0–512 μM), TAX (0–32 nM), DOC (0–1600 nM) as single agents. As to Siha cells treated for 48 h with either CDDP (0–80 μM), CBP (0–1200 μM), NDP (0–320 μM), LBP (0–120 μM), OXA (0–640 μM), TAX (0–5160 nM),

DOC (0–400 nM). Finally, U14 cells were treated for 24 h with either DDP (0–40 μM), CBP (0–1200 μM), NDP (0–160 μM), LBP (0–120 μM), OXA (0–640 μM), TAX (0–8000 nM), DOC (0–200 nM) as single agents. After treatment, cell counting kit-8 (CCK-8) at 10 μL/well (Dojindo; C0042, Kumamoto, Japan) added for incubation for two hours, and the absorbance measured at 450 nm with a microplate reader (Molecular Devices, Sunnyvale, CA, USA). The inhibitory concentration (IC) of the drug that leads to 50% (IC₅₀) growth inhibition was calculated using the software GraphPad Prism 9.0.0 (9.0.0121) (Dotmatics, Boston, MA, USA). All experiments were performed at least in triplicate. For ECA109 and Siha cells, the treatment was 48 h, while U14 treated for 24 h.

2.3 Cell Apoptosis Detection

After culture and treatments, cells were collected and centrifuged at 1000 g for 5 min. Then, the cells in 195 μL binding buffer were incubated with 5 μL AnnexinV-Fluorescein Isothiocyanate (FITC) and 10 μL PI for 15 min at room temperature in the dark according to the manufacturer’s instruction (Beyotime, C1062S, Shanghai, China). Cell apoptosis was analyzed by flow cytometer.

2.4 ATP Release

Extracellular ATP was measured in the conditioned media (supplemented with heat inactivated FBS) 24 h after chemotherapeutic treatment using the Firefly luciferase ATP assay, according to the manufacturer’s protocol (Beyotime, S20026, Shanghai, China). The bioluminescent signal was measured using a SpectarMaxL plate reader (Molecular Devices, Sunnyvale, CA, USA).

2.5 HMGB1 Release

Release of HMGB1 was analyzed 48 h after treatment in the conditioned media using an enzyme-linked immunosorbent assay kit (Animaluni, Human: LV10792, Mouse: LV30652, Shanghai, China) according to the instructions of the manufacturer. The absorption was measured via the SpectarMax iD3 plate reader (Molecular Devices, Sunnyvale, CA, USA).

2.6 Detection of Damps Molecule in Condition Media via Western Blot

After culture and treatments, condition media collected by Laboratory Syringe Filters (Merck; SLGPR33RB, Rahway, NJ, USA). It should be noted that the media used to detect supernatant proteins were Serum-free media, this is due to the fact that only Serum-free media can ensure that no other proteins interfere with the collected supernatant. Since the damps molecule itself is minimally expressed in the supernatant, we innovatively used a gradient of drug concentrations in order to be able to observe more significant changes. Briefly, we set the concentration of each drug treated for three cell lines to 0.5 × IC₅₀, 1 × IC₅₀,

$2 \times \text{IC}_{50}$, $4 \times \text{IC}_{50}$, $8 \times \text{IC}_{50}$ based on the IC_{50} values of each drug (**Supplementary Tables 1,2,3**) in different cells determined in the previous period. First, we quantified the amount of protein loaded in each lane utilizing the silver staining kit (Thermo; 24612, Waltham, MA, USA) following the manufacturer's protocol (**Supplementary Fig. 1**). Next, Supernatant protein samples (20 μL) were separated by SDS-PAGE (Ace; ET15420Gel, Changzhou, China) and transferred to polyvinylidene fluoride (PVDF) membranes. Next, the membranes were blocked with 10% non-fat milk for one hour and incubated overnight at 4 °C with primary antibodies: HSP70 (Cell Signaling; 4872T, Danvers, MA, USA), CRT (Cell Signaling; 12238S, Danvers, MA, USA), Annexin A1 (ANXA 1) (Abcam; ab214486, Cambridge, UK), HMGB1 (Abcam; ab79823, Cambridge, UK). Finally, the membranes were incubated with HRP-conjugated secondary antibodies (Bio-Rad, 1706515, Hercules, CA, USA) at room temperature for one hour. Western blotting analysis was performed using a Bio-Rad chemiluminescence imager (Bio-Rad, Hercules, CA, USA). At last, we performed a grayscale analysis of the individual western-blot bands using the image-lab software (3.0.39529, Bio-Rad, Hercules, CA, USA) and heat maps were drawn by the software GraphPad Prism 9.0.0 (9.0.0121) (Dotmatics, Boston, MA, USA).

2.7 *In Vivo* Vaccination Assay

We used the classical *in vivo* experimental model of ICD detection experiment [13]. Concisely, Six-week-old female C57BL/6J wild-type mice were used to generate experimental tumors by grafting a mouse cervical carcinoma cell line (U14). Mice were injected in the groin, according to the experiment, with 2×10^6 U14-control cells and U14-drug handling cells, single IC_{50} concentration for 24 hours. After seven days, On the contralateral side, we injected the same number of tumor cells without any treatment. On days 1, 4, 7...28, the tumor volume was measured every three days using the following formula: $\text{Tumor volume (mm}^3\text{)} = 0.5 \times \text{width}^2 \times \text{length}$. At the end of the experiment, mouse ocular blood collected after anaesthesia with Delivector™ Avertin (20 $\mu\text{L/g.ip}$) (DW3101, Dowobio, Shanghai, China) and tumors retained for subsequent experiments. Mice are euthanized by way of cervical subluxation when reaching their ethical endpoint (volume $>1500 \text{ mm}^3$ or deep ulceration).

2.8 Immunohistochemistry Assays

Tumor tissues prepared as 3 μm thick paraffin sections. For Immunohistochemistry (IHC) staining, the slides were dewaxed with xylene (Sangon Biotech, A530011, Shanghai, China) and rehydrated using graded ethanol (Sangon Biotech, A507050, Shanghai, China). Autoclaved antigen retrieval was performed in sodium citrate HCl buffer (Yun Tai, YTH0057, Shanghai, China), an endogenous H_2O_2 (Sangon Biotech, A001896, Shanghai, China)

enzyme blocker (MXB, SP KIT-A3, Fuzhou, China) was used to block the tissues for 10 min, and 5% goat Serum (Sangon Biotech, E510009, Shanghai, China) was used for blocking at 37 °C for 1 h. The sections were incubated at 4 °C overnight with primary antibodies: anti-CRT rabbit antibody (1:250, Abcam; ab92516, Cambridge, UK), HMGB1 rabbit antibody (1:350, Abcam; ab79823, Cambridge, UK). The HRP-conjugated secondary antibody (Abcam, ab6728, Cambridge, UK) was incubated with the sections for 30 min at 37 °C. The sections were rinsed with PBS (Pricella; PB180327, Wuhan, China), developed with diaminobenzidine substrate (Abcam, ab64238, Cambridge, UK), and counter-stained with hematoxylin (Abcam, ab220365, Cambridge, UK) for nuclear staining. A light microscope used to observe and capture images of the histopathological changes.

2.9 Enzyme-Linked Immunoassay for Serum DAMPS

Mouse sera obtained from the *in vivo* experiments described above, and all experimental steps performed in strict accordance with the kit operating instructions. The DAMPs molecules detected include HSP70 (Animaluni; LV30721, Shanghai, China), CRT (Animaluni; LV31001, Shanghai, China), ANXA 1 (Animaluni; LV31010, Shanghai, China), and HMGB1 (Animaluni; LV30652, Shanghai, China).

2.10 Patients and Samples

Eight patients with histologically diagnosed primary squamous carcinoma who treated at the Oncology Center of the Third Affiliated Hospital of Army Military Medical University selected for the study (**Supplementary Table 4**). All patients were diagnosed for the first time and did not receive any other treatment regimen, and this time, they treated according to a combination regimen of platinum in combination with a taxanes. To evaluate the promotional effect of the chemotherapy regimen on the DAMPs molecule, we collect peripheral blood from the patients before and during the first cycle after treatment. Serum obtained by high-speed cryo-centrifugation (4 °C 1.5×10^4 rpm) for enzyme linked immunosorbent assay (ELISA). Detection of HSP70 (Animaluni; LV10661, Shanghai, China), CRT (Animaluni; LV11352, Shanghai, China), ANXA 1 (Animaluni; LV11124, Shanghai, China), and HMGB1 (Animaluni; LV10792, Shanghai, China) in Serum carried out according to the kit instructions. This study and the use of all clinical materials were approved by the individual Institutional Ethical Committees, and written informed consent was obtained from all participant.

2.11 Statistical Analysis

Statistical data expressed as mean \pm standard deviation (SD). One-way analysis of variance used for three groups and more than three groups. All of the statistical analyses assessed by software GraphPad Prism (GraphPad Software, Inc., SanDiego, CA, USA), comparisons among

Table 1. IC50 of chemotherapeutic drugs in ECA109 cells.

Agent	IC50 (95% CI)	DOF	R ²
DDP	0.9782 (0.8763–1.090) μM	38	0.9656
CBP	35.56 (31.71–39.881) μM	25	0.9801
NDP	4.712 (4.342–5.100) μM	26	0.9773
LBP	8.233 (7.4–9.155) μM	26	0.9779
OXA	12.36 (9.14–16.30) μM	25	0.8931
TAX	5.673 (4.92–6.555) nM	19	0.9600
DOC	59.45 (10.12–85.9) nM	19	0.9163

DDP, cisplatin; CBP, carboplatin; NDP, nedaplatin; LBP, lobaplatin; OXA, oxaliplatin; TAX, paclitaxel; DOC, docetaxel; IC50, half-maximal inhibitory concentration; CI, confidence interval; DOF, Degree of Freedom.

Table 2. IC50 of chemotherapeutic drugs in SIHA cells.

Agent	IC50 (95% CI)	DOF	R ²
DDP	8.766 (7.984–9.624) μM	34	0.9716
CBP	190.8 (172.8–210.7) μM	29	0.9631
NDP	32.01 (29.70–34.49) μM	29	0.9771
LBP	21.66 (19.90–23.55) μM	28	0.9727
OXA	19.58 (17.66–21.80) μM	22	0.9829
TAX	1582 (1267–1987) nM	16	0.9147
DOC	62.05 (37.12–105.5) nM	16	0.9064

groups were done by the independent sample two-sided Student *t*-test. The ANOVA performed to evaluate the statistical differences among groups. *p*-value of 0.05 or less considered as statistical significance.

3. Results

3.1 Evaluation of the Cytotoxic Effects of Various Chemotherapeutic Agents on SCC Cell Lines

First, we evaluated the dose-response curves of commonly used TP regimen drugs, namely DDP, CBP, NDP, LBP and OXA, and the taxanes DOC and TAX, in the human SCC cell lines ECA109 and SIHA, and in the mouse cervical SCC cell line U14 (**Supplementary Fig. 2A–C**). Due to the varying sensitivities of the three SCC cell lines to the chemotherapy agents, different IC50 values were used in subsequent experiments. The most effective drug inhibitory effect in the human SCC lines ECA109 and SIHA occurred after 48 h. In contrast, each drug had a noticeable inhibitory effect on the growth of mouse cervical SCC U14 cells after just 24 h, indicating greater sensitivity of these cells to the drugs. The IC50 values for each chemotherapeutic drug are shown in Tables 1,2,3 for the three SCC cell lines.

3.2 Release of Damage-Associated Molecular Patterns (DAMPs) from SCC Cell Lines Following Treatment with Chemotherapeutic Agents

To determine the optimal drug concentration for inducing the extracellular release of DAMPs, a gradient treat-

Table 3. IC50 of chemotherapeutic drugs in U14 cells.

Agent	IC50 (95% CI)	DOF	R ²
DDP	3.968 (3.766–4180) μM	22	0.9902
CBP	104.8 (96.19–114.1) μM	25	0.9861
NDP	24.54 (23.11–26.04) μM	22	0.9915
LBP	13.27 (12.81–13.75) μM	43	0.9947
OXA	7.693 (6.98–8.46) μM	38	0.9773
TAX	199.1 (129.2–297.2) nM	22	0.9348
DOC	13.71 (12.16–15.44) nM	22	0.9811

ment approach was employed in which the concentration of each drug was varied. Subsequently, a quantitative assay was used to measure the level of extracellular DAMPs in the supernatants of the three SCC cell lines following treatment with the chemotherapeutic agents. Based on our earlier findings, the supernatant proteins were collected after 48 h of treatment in the ECA109 and SIHA cell lines, and after 24 h of treatment in the U14 cell line.

3.3 The Release of DAMPs by SCC Cell Lines Following Treatment with Platinum Drugs

Previous studies have shown that OXA induced ICD in colorectal tumor cells [14,15]. However, the role of OXA in esophageal SCC and cervical SCC has yet to be systematically investigated. Here, we found that all three generations of platinum drugs induced release of the DAMP molecules HSP70, ANXA1, HMGB1 and CRT in a dose-dependent manner in the ECA109 cell line (Fig. 1A). The first-generation platinum drug DDP strongly induced the extracellular release of HSP70, ANXA1 and HMGB1. However, CRT induction primarily involved its displacement from the endoplasmic reticulum to the periplasm. The third-generation platinum drug OXA showed comparable results to DDP, with strong induction of HSP70, ANXA1 and HMGB1 release, but limited impact on CRT. However, the second-generation platinum drugs CBP and NDP induced a noticeable release of all four DAMP molecules. CBP induced the highest release at the drug's half-maximal inhibitory concentration (IC50). Subsequently, the release of DAMP molecules gradually decreased, with HSP70 showing the most reduction. On the other hand, low doses of the third-generation platinum drug LBP induced limited extracellular release of HSP70 and ANXA1. However, a pronounced dose-dependent effect of LBP was observed at twice the IC50 concentration. Similarly, low doses of LBP induced noticeable extracellular release of CRT and HMGB1, with their release peaking at twice the IC50 concentration.

All three generations of platinum drugs induced the release of DAMP molecules from SIHA cells in a dose-dependent manner (Fig. 1B). However, several of the platinum drugs showed weaker induction of extracellular DAMP release from SIHA cells compared to ECA109 cells. In particular, the first-generation drug DDP and the second-

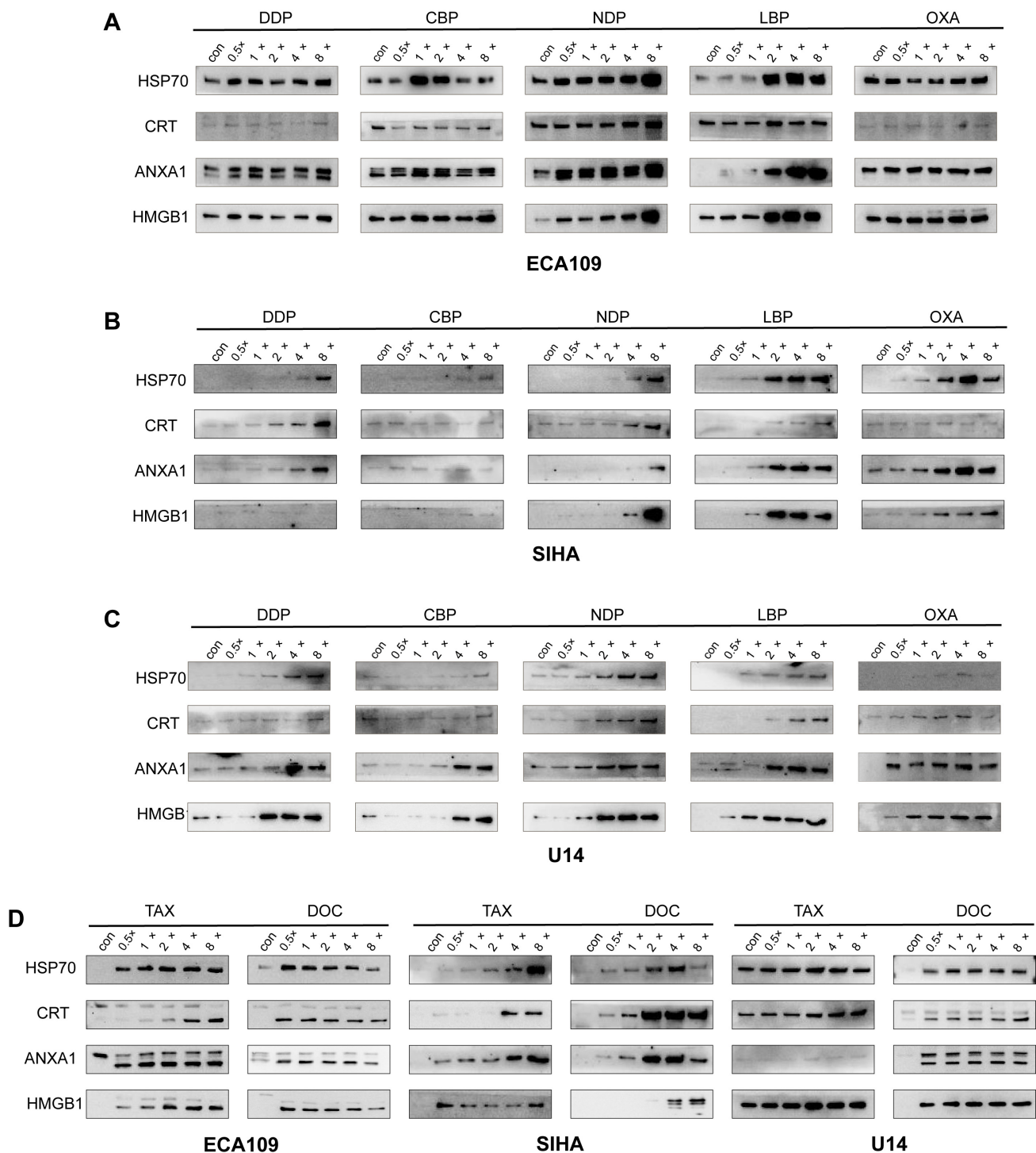


Fig. 1. Release of HSP70, CRT, ANXA1 and HMGB1 from SCC cell lines after treatment with chemotherapy drugs. (A) Release of HSP70, CRT, ANXA1 and HMGB1 into the supernatant after treatment of ECA109 cells with platinum-based chemotherapeutic agents for 48 h. (B) Release of HSP70, CRT, ANXA1 and HMGB1 into the supernatant after treatment of SIHA cells with platinum-based chemotherapeutic agents for 48 h. (C) Release of HSP70, CRT, ANXA1 and HMGB1 into the supernatant after treatment of U14 cells with platinum-based chemotherapeutic agents for 24 h. (D) Release of HSP70, CRT, ANXA1 and HMGB1 into the supernatant of ECA109, SIHA and U14 cells after treatment with taxane-based chemotherapeutic agents for 48 h or 24 h. HSP70, Heat Shock Protein 70; CRT, Calreticulin; ANXA1, membrane-connected protein A1; HMGB1, High Mobility Group Protein B1; SCC, squamous cell carcinoma.

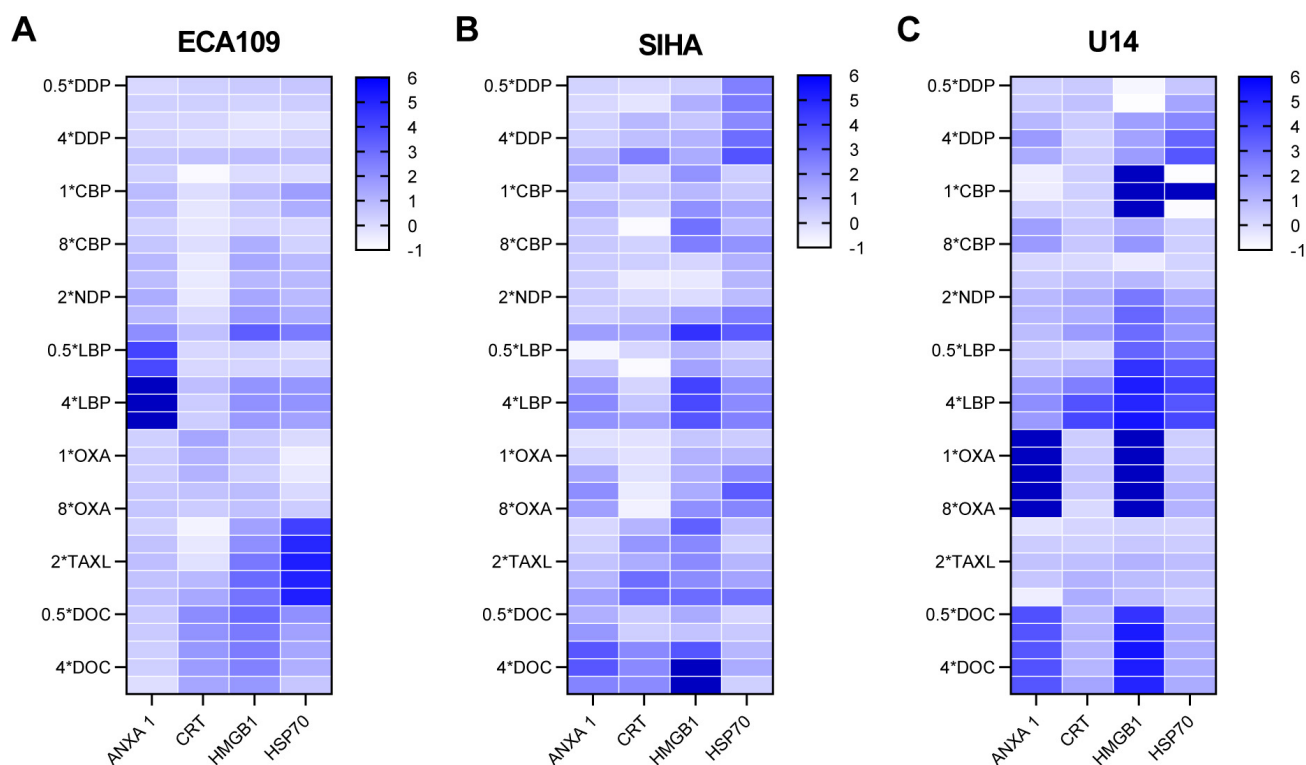


Fig. 2. Overview of the normalized values of DAMPs released from the SCC cell lines. (A) ECA109 cells. (B) SIHA cells. (C) U14 cells. DAMPs, damage-associated molecular patterns.

generation drugs CBP and NDP induced less release of extracellular DAMP molecules from SIHA cells compared to ECA 109 cells. In contrast, the third-generation drugs LBP and OXA showed markedly stronger effects in SIHA cells. A more precise representation is provided by the heat map analysis shown in Fig. 2. Among the three generations of platinum drugs, DDP strongly induced the extracellular release of CRT and ANXA1, whereas CBP and NDP showed only limited induction of DAMP release. Both of the third-generation drugs, LBP and OXA, induced strong release of DAMPs, with the exception of CRT.

To further examine the effect of ICD *in vivo*, we evaluated the extracellular release of DAMPs in mouse cervical SCC U14 cells following treatment with platinum drugs. These induced a more pronounced extracellular release in mouse U14 cells compared to SIHA cells (Fig. 1C). Of note, DDP and CBP showed stronger effects on the release of ANXA1 and HMGB1 compared to HSP70 and CRT in U14 cells. NDP had a significant impact on DAMP release, particularly on ANXA1, although the threshold value was reached at twice the IC50 concentration. Overall, LBP had a greater effect on the release of DAMPs compared to OXA. Treatment with LBP at the IC50 concentration led to a pronounced release, particularly for HMGB1, whereas OXA treatment resulted in a significant release of CRT only. The relatively weak induction of CRT observed in the three cell lines may be due to its dual functions. It is generally believed that ecto-CRT can induce ICD in its role

as a DAMP. As noted previously, CRT was included as a molecular signature for ICD. However, the presence of CRT in extracellular spaces may also promote or recognition by Antigen-presenting cells (APC), thereby contributing to immunological surveillance [16]. Research has shown that the serum CRT level is highly correlated with patient prognosis [17]. Therefore, in order to be more relevant to clinical practice, we chose to detect CRT in the supernatant. Moreover, the expression of ecto-CRT is temporally related, reaching a peak at 48 h and then only gradually increasing in the extracellular space following tumor cell apoptosis [18].

3.4 DAMP Release by SCC Lines after Treatment with Taxane Drugs

We next evaluated the effect of taxane drugs on the extracellular release of DAMPs in the three SCC cell lines. These drugs induced significant extracellular release of DAMPs in all cell lines (Fig. 1D). However, in SIHA cells the release of CRT was not observed until the dose reached four times the IC50 concentration. DOC showed a diversity of induction across the different cell lines. ECA109 cells showed a peak in the extracellular release of DAMPs at half the IC50 concentration, suggesting high sensitivity to DOC. In contrast, the DOC-induced release of HMGB1 was relatively low in SIHA cells, with release only observed at four times the IC50 concentration. For other DAMP molecules, the peak effect on release was observed at four times the

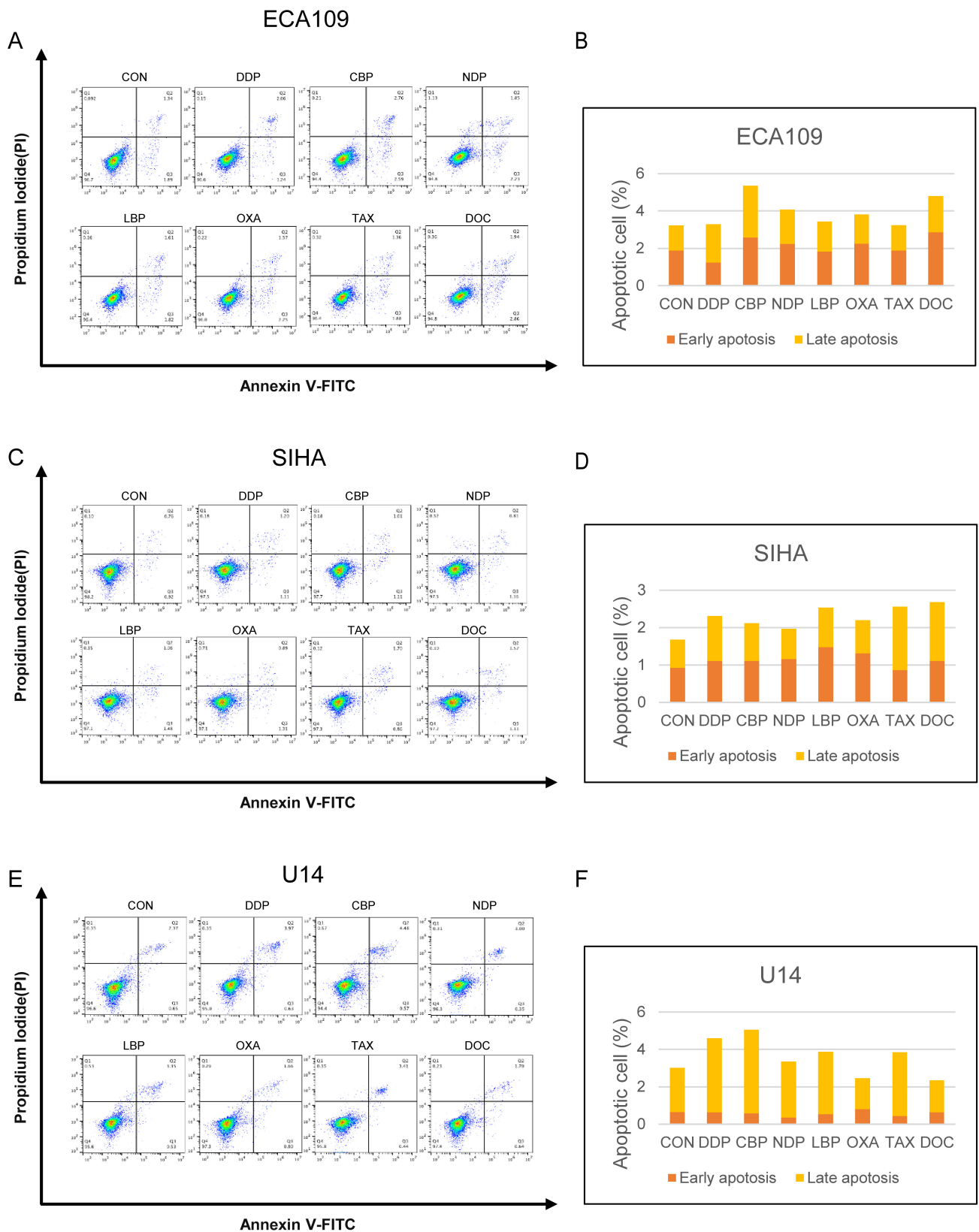


Fig. 3. Detection of apoptosis following treatment with different chemotherapeutic drugs. (A) Detection of apoptosis in ECA109 cells following treatment with platinum-based drugs and taxane. (B) Proportion of ECA109 cells showing early apoptosis and late apoptosis. (C) Detection of apoptosis in SIHA cells following treatment with platinum-based drugs and taxanes. (D) Proportion of SIHA cells showing early apoptosis and late apoptosis. (E) Detection of apoptosis in U14 cells following treatment with platinum-based drugs and taxanes. (F) Proportion of U14 cells showing early apoptosis and late apoptosis.

IC50 concentration, followed by a decrease at higher concentrations. A specific threshold effect of DOC may account for this observation in SIHA cells. U14 cells showed comparable results to ECA109 cells, with the peak release of DAMPs occurring at a low drug concentration ($0.5 \times$ IC50). No significant release was observed at higher concentrations.

In summary, the specific induction pattern of each DAMP molecule varied with each drug, while the optimal concentration for induction also differed. However, almost all drugs induced the extracellular release of DAMP molecules.

3.5 Overview of DAMPs Following Treatment of SCC Cell Lines with Chemotherapy Drugs

To visually represent the release of extracellular DAMPs following treatment with each drug, we conducted a grey value analysis of the western blot images shown in Fig. 1. The release of DAMPs from each group was logarithmically transformed using a reference value of one for the blank control. A comprehensive evaluation of the release of DAMPs from the three SCC cell lines is shown in Fig. 2. The selected human and murine SCC cell lines demonstrated significantly elevated levels of HSP70, CRT, ANXA1 and HMGB1 compared to the control group. The release of DAMPs varied according to treatment with either first-, second- or third-generation platinum-based and taxane-based agents. Importantly, the platinum-based agents elicited significantly greater release of DAMPs from esophageal SCC compared to cervical SCC. Additionally, higher doses of platinum-based drugs were required to induce ICD in both the human and murine cervical SCC cell lines.

3.6 The Impact of Platinum and Paclitaxel Agents on Apoptosis

ICD as a type of regulated cell death that differs from other forms of cell death such as apoptosis, ferroptosis, and necroptosis [19]. We conducted apoptosis assays based on the optimal drug concentrations for induction determined previously. The results are shown in Fig. 3, and changes in cell morphology are documented in **Supplementary Fig. 3**. The interaction of optimal drug concentrations resulted in a lower proportion of cells in the apoptotic phase, suggesting that ICD is not a straightforward form of apoptosis.

3.7 ATP Secretion

We next performed an ATP assay to quantify the release of ATP in conditioned media following treatment of the three SCC cell lines for 24 h with each chemotherapeutic agent. A consistent inhibitory effect of LBP and TAX on the release of ATP was observed in all three cell lines (Fig. 4).

Both CBP and DOC induced a significant increase in the secretion of ATP in ECA109 cells, with an approx-

imately 1.5-fold increase compared to the control group (Fig. 4A). OXA caused a slight increase, while DDP and NDP did not induce ATP release. DDP, OXA and DOC induced more release of ATP from SIHA cells compared to CBP and NDP, with the latter two showing minimal ability to induce ATP release (Fig. 4B). Finally, NDP, OXA, and DOC induced significant release of ATP from the U14 cell line compared to the control group (Fig. 4C). In summary, OXA and DOC demonstrated superior induction of ATP release from SCC cell lines.

3.8 Release of HMGB1

HMGB1 is known to stabilize DAMPs. We quantified its release from SCC cells using ELISA (Fig. 5). U14 cells were treated with the chemotherapy drugs for 24 h, while ECA109 and SIHA cells were treated for 48 h before collection of the supernatants for analysis. Consistent with the previous findings, significant release of HMGB1 from all three cell lines was observed following drug treatment compared to the control group.

3.9 *In Vivo* Vaccination Assay of U14 Cells in a Mouse Model

In vitro experiments can provide valuable insights into the potential for therapeutic agents to elicit an effective anti-tumor immune response. However, these assays do not take into consideration the complete immune system. To study this, we conducted a vaccination experiment as described earlier. The weight of all mice remained stable throughout the experiment. Fig. 6 illustrates the percentage of tumor-free mice, the rate of tumor growth, and representative tumors *in vivo*.

All five mice (100%) in the control group vaccinated with untreated cells developed a tumor at the challenge site. In contrast, none of the mice (0%) vaccinated with cells treated with DDP, DOC, NDP or OXA developed a tumor at the challenge site (Fig. 6B–D). Sixty percent of mice vaccinated with carboplatin-treated cells showed tumor development, whereas all mice (100%) vaccinated with LBP- or TAX-treated cells developed a tumor (Fig. 6B–D). Furthermore, at the end of the experiment the tumor volume in the DDP, CBP, NDP, OXA and DOC vaccinated groups was significantly larger than in the control group (Fig. 6E). This result suggests that DDP, CBP, NDP, OXA and DOC are able to induce ICD in mice with cervical SCC.

To further validate and identify the critical molecules involved in ICD, the concentrations of DAMP molecules were evaluated in the Serum of experimental mice (Fig. 7A). DDP was found to induce comparable levels of HSP70, ANXA1 and CRT release into the Serum as the previous *in vitro* experiments conducted at the cellular level. The known inducer of ICD, OXA, also induced high levels of HSP70, ANXA1, CRT and HMGB1 secretion into the Serum of mice treated with this drug, thus further confirming its effect on ICD in SCC. Mice treated with CBP, NDP

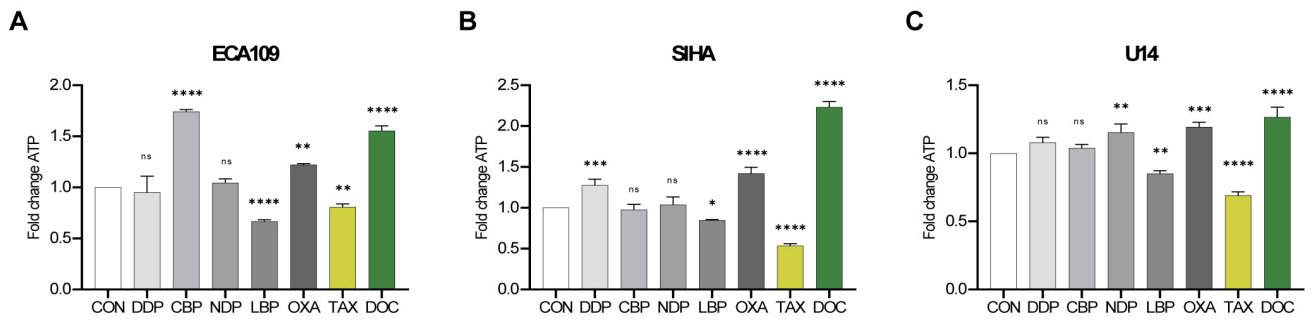


Fig. 4. Adenosine triphosphate (ATP) release from SCC cell lines after treatment with chemotherapy drugs. The release of ATP from ECA109, SIHA and U14 cells was assessed after 24 h of treatment with the IC₅₀ dose for DDP, CBP, NDP, LBP, OXA, TAX and DOC. (A) ECA109 cells. (B) SIHA cells. (C) U14 cells. Error bars represent the standard deviation. Experiments were performed at least in triplicate. ns $p > 0.05$, * $p < 0.05$, ** $p < 0.01$, *** $p < 0.001$, **** $p < 0.0001$.

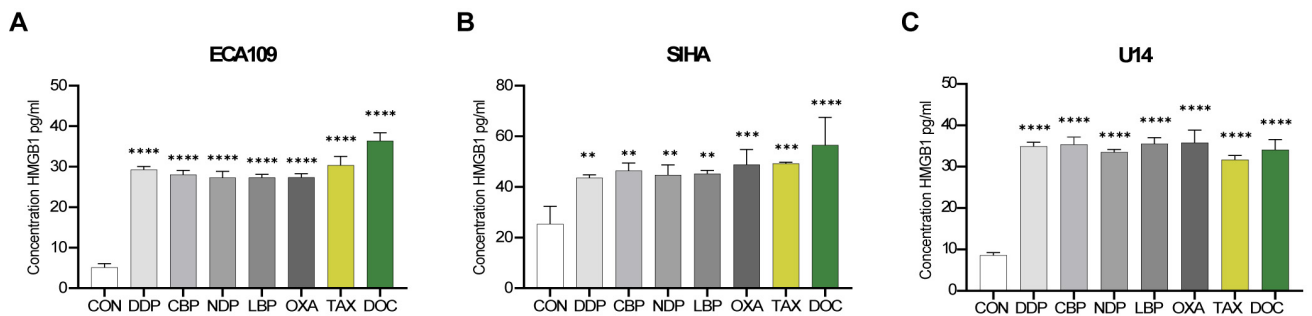


Fig. 5. Release of high mobility group protein B1 (HMGB1) from SCC cell lines following chemotherapy drug treatment. HMGB1 (pg/mL) in the supernatant was assessed after 48 h of treatment of the ECA109 and SIHA cells, and after 24 h of treatment of the U14 cells. The IC₅₀ dose was used for DDP, CBP, NDP, LBP, OXA, TAX and DOC. (A) ECA109 cells. (B) SIHA cells. (C) U14 cells. ** $p < 0.01$, *** $p < 0.001$, **** $p < 0.0001$. Error bars represent the standard deviation. Experiments were performed in triplicate.

or DOC showed significant release of DAMPs, consistent with the results of earlier *in vitro* experiments. In contrast, LBP and TAX are unable to induce ICD and did not show any significant release of the four DAMP molecules in this mouse model. Although LBP and TAX induced some extracellular release of DAMPs *in vitro*, they were unable to induce ICD in the complexity of an *in vivo* environment.

Immunohistochemical evaluation of tumor cells at the site of reinoculation confirmed the Serum test results (Fig. 7B). In the control group, CRT was found to be exclusively intracellular, while HMGB1 was confined to the nucleus, indicating they were unable to induce ICD. In contrast, LBP- and TAX-treated mice showed low expression of these molecules, possibly indicating depletion and insufficient downstream ICD effects. However, CBP-treated mice showed high expression of both CRT and HMGB1, thus confirming the ability of this agent to induce ICD.

3.10 Serum Samples from SCC Patients Contain Elevated Levels of CRT and HMGB1

DAMPs are typically released at high levels from various types of cancers, including SCC. To extend the current observations on the increased release of DAMPs following chemotherapeutic drug treatment of SCC cell lines,

we used ELISA to determine the Serum levels of DAMPs in 8 SCC patients before and after chemotherapy. In four patients, the Serum concentrations of HSP70, CRT, ANXA1 and HMGB1 were significantly higher post-chemotherapy compared to the Pre-chemotherapy SCC patients (Fig. 8A). The other four patients showed increased Serum levels of different DAMPs following chemotherapy. Further analysis revealed that increased DAMP levels were associated with chemotherapeutic stimulation in SCC (Fig. 8B).

4. Discussion

The induction of immunogenic cell death (ICD) by chemotherapy has been extensively studied both *in vitro* and *in vivo* [15]. The earliest research on immune therapy for tumors can be traced back to the 19th century [16]. The literature on ICD in tumor biology has expanded significantly over the past few years, providing new possibilities for cancer treatment. With the increased research on ICD, more and more clinical drugs and treatment methods are now recognized as having ICD-inducing effects. Moreover, immunotherapy is gradually being combined with conventional treatments to combat drug resistance. However, due to the toxicity and absorption issues associated with drugs, it is often difficult to effectively induce ICD.

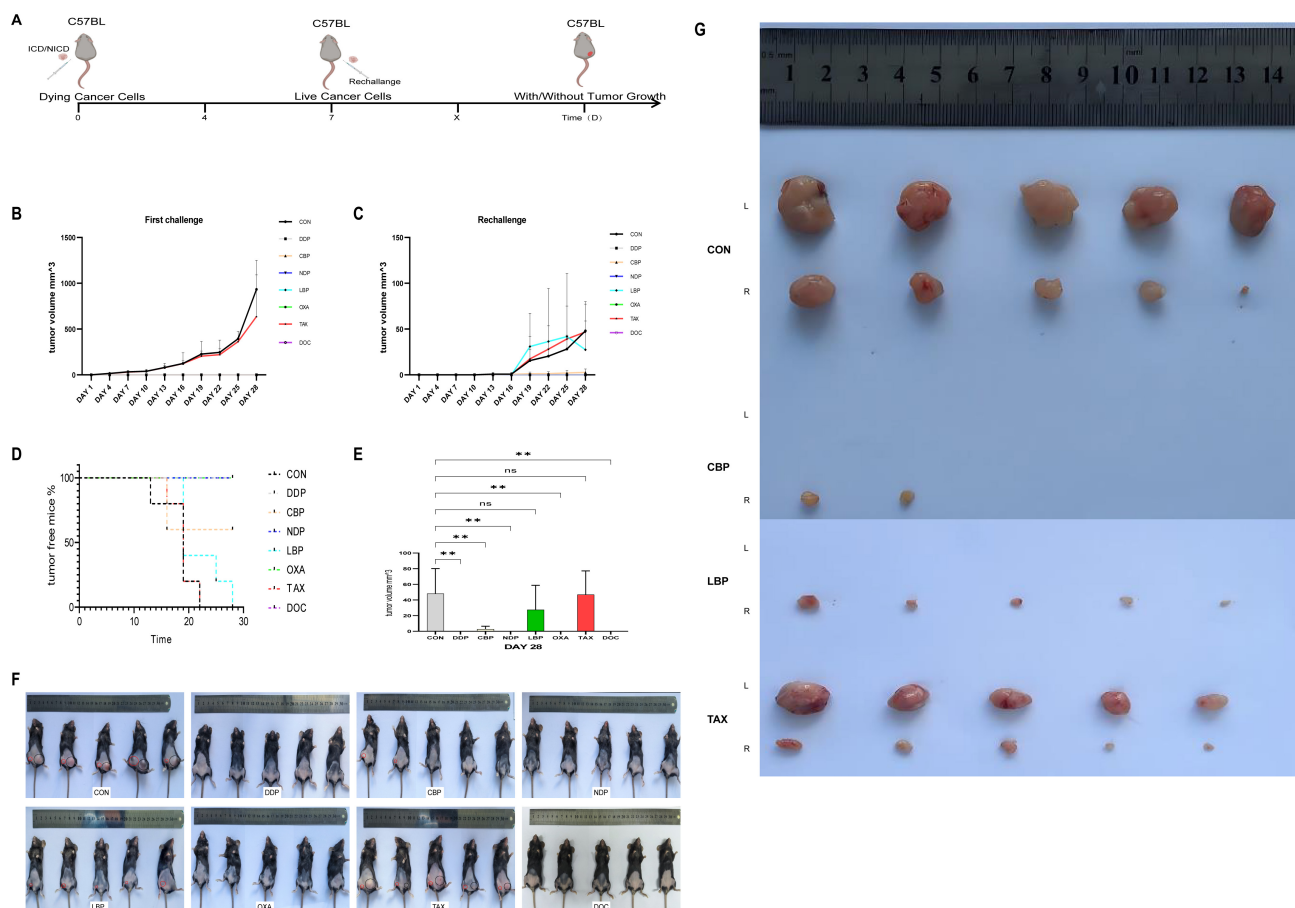


Fig. 6. *In vivo* vaccination in the C57BL/6J mouse model underscores the immunogenic ability of clinically relevant chemotherapeutics. (A) Schematic diagram of the experimental protocol. (B) Tumor volumes in the xenograft model were measured every three days and are shown at the challenge site. (C) Tumor volumes in the xenograft model were measured every three days and are shown at the rechallenge site. (D) Percentage (%) of tumor-free mice and tumor volume (mm^3) in C57BL/6J mice at 28 days. (E) Tumor volume at the rechallenge site in each treatment group after normalization. Quantitative data from three independent experiments are shown as the mean \pm standard deviation (SD) (error bars). ns $p > 0.05$, $**p < 0.01$. (F) Tumors at the challenge and rechallenge sites on day 28 are shown in the control mice and in mice treated with DDP, CBP, NDP, LBP, OXA, TAX or DOC. (G) *In vivo* vaccination showing the immunogenic potential of clinically relevant chemotherapeutic drugs in the mouse model with U14 cells. Resected tumors from the challenge and rechallenge sites at day 28 are shown from the controls and from mice treated with CBP, LBP or TAX. ICD, immunogenic cell death inducer; NICD, non-immunogenic cell death inducer.

Therefore, some researchers have proposed direct delivery of ICD-inducing agents or DAMP molecules to the vicinity of tumor tissues in order to more efficiently induce ICD [16]. Research on new ICD inducers has also continued, and natural compounds that act as ICD inducers could represent a new frontier in cancer therapy. Among these, various plant-derived molecules, marine molecules, and bacteria-based compounds may be suitable for inducing ICD [20]. However, to date there has been no systematic research on platinum- and taxane-based drugs, and research on nedaplatin and lobaplatin has been neglected [7]. The current research therefore provides a systematic and comprehensive analysis of the ICD induction effects of three generations of platinum drugs and two generations of paclitaxel drugs. As mentioned earlier, DAMP molecules play

an important role in the induction of ICD. During the initial stages, translocation of CRT and exposure at the cell surface triggers a robust anti-tumor immune response. Expression of CRT at the cell surface displays an “eat me” signal that is recognized and phagocytosed by CD91. This promotes dendritic cell (DC) maturation and activation, leading to the generation of tumor antigens and tumor-specific activation [7]. During the mid-apoptosis stage, HSP70 facilitates the release of pro-inflammatory cytokines, increases the expression of co-stimulatory molecules, and together with other immune molecules regulates immune function. During the ICD response in tumor cells, antigens bind to HSP70 to form a complex, thereby stimulating the uptake of tumor antigens and the maturation and activation of DCs and NK cells. HSP70 binds to the costimulatory molecule

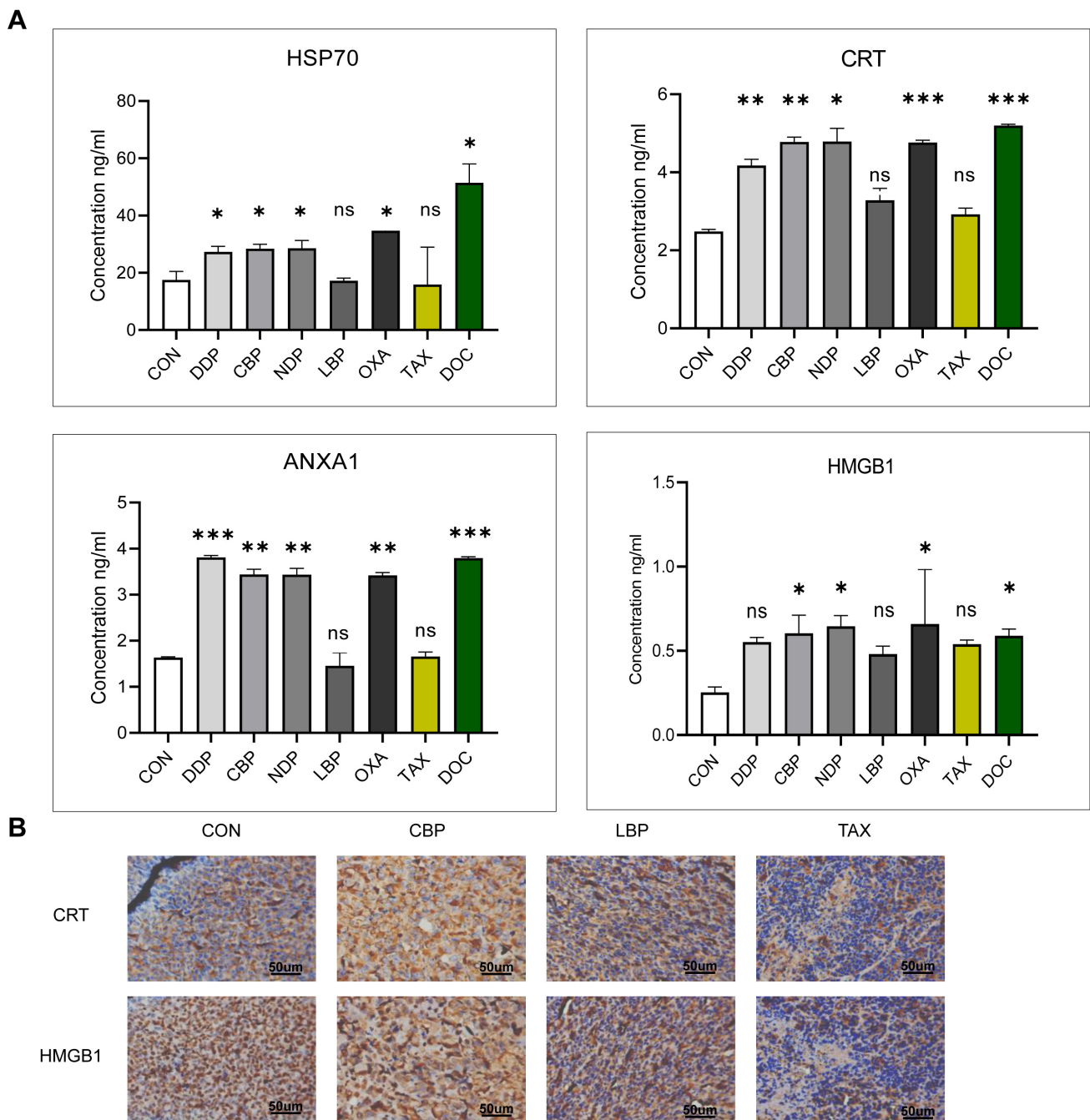


Fig. 7. Release of DAMP molecules into mouse Serum and tumor tissues. (A) Serum levels of HSP70, ANXA1, CRT, and HMGB1 in C57BL/6J mice treated with chemotherapeutic agents. (B) Immunohistochemical study of CRT and HMGB1 expression and their intracellular localization in representative xenograft tumors (400 \times magnification, scale bar = 50 μ m). Quantitative data from three independent experiments are shown as the mean \pm SD (error bars). ns $p > 0.05$, * $p < 0.05$, ** $p < 0.01$, *** $p < 0.001$.

CD40 to activate cytotoxic T lymphocytes [7]. HMGB1 is released from the cell and binds to pattern recognition receptors (PRR), subsequently activating monocytes and macrophages to release pro-inflammatory cytokines and enhancing antigen presentation by DCs during the late apoptotic stage [7]. Similarly, ANXA1 appears to act as a homing factor that plays a non-redundant role in regulating the pathway through which DCs or their precursors ultimately

infiltrate tumor cells during ICD [7]. ATP is released from the cell via ATP-containing vesicles. The ATP content varies and its activated receptors are also different. When the amount of ATP released from the cell is low, ATP can activate the P2Y2 receptor to send a “find me” signal to DCs and macrophages, thereby promoting DC activation and maturation, as well as the expansion of macrophages [21]. On the other hand, ATP can also activate P2X7 and

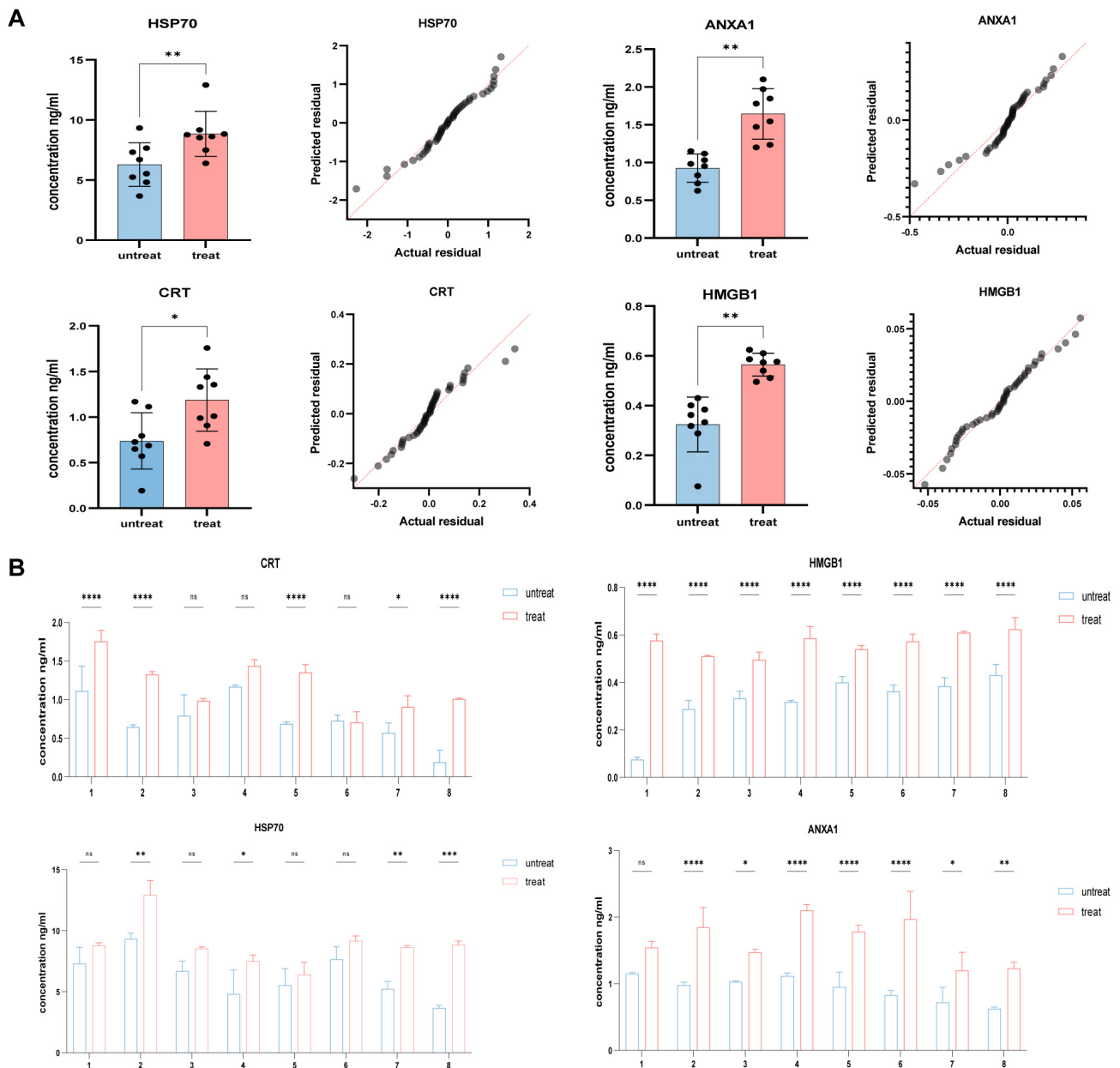


Fig. 8. Elevated Serum levels of CRT and HMGB1 after chemotherapeutic stimulation in SCC patients. (A) Post-chemotherapy Serum levels of HSP70, CRT, ANXA1 and HMGB1 were significantly higher in four SCC patients compared to non-chemotherapy controls, as measured by ELISA. (B) Serum levels of HSP70, CRT, ANXA1 and HMGB1 in non-chemotherapy controls and in 8 post-chemotherapy SCC patients, as measured by ELISA. Quantitative data from three independent experiments are shown as the mean \pm SD (error bars). ns $p > 0.05$, $*p < 0.05$, $**p < 0.01$, $***p < 0.001$, $****p < 0.0001$. ELISA, enzyme-linked immunosorbent assay.

the P2X7 receptor can subsequently activate cytotoxic T lymphocytes [22]. HMGB1, CRT, HSP70 and ANXA1 are all DAMP molecules that play crucial roles in cell signaling and in the immune response. It has been suggested that *Trametes robiniophila* Murr (Huaier) induces ICD in triple-negative breast cancer cells by promoting the exposure of CRT, increasing the release of ATP and HMGB1, and triggering the release of DAMPs [23]. This interaction may contribute to intracellular signaling and immune modulation. The Hsp70-HMGB1 complex present in the extracel-

lular matrix could potentially serve as a marker for cancer recurrence. This complex is found in conditioned medium and interacts with other factors, leading to enhanced expression of proliferation markers, activation of autophagy, and increased production of prostaglandin E, all of which contribute to tumor growth. Inhibition of the Hsp70-HMGB1 complex shows promise for the treatment of cancers with a high risk of relapse [24]. The appropriate application of amplitude-modulated radiofrequency (amRF) has been shown to enhance the anti-tumor activity of HSP. amRF

also promotes the secretion of HSP70 into the extracellular matrix. Together, extracellular HSP70 accompanied by free HMGB1 and membrane-expressed CRT are DAMPs that encourage DC maturation for antigen presentation [25]. Moreover, it was previously reported that HSP70 and c-Jun N-terminal kinase (JNK) may be involved in heat stress and inflammatory stress responses regulated by ANXA1. This interaction could influence the immune response and the regulation of inflammation [26]. In summary, interactions between HMGB1, CRT, HSP70 and ANXA1 are involved in the coordination of immune responses, tissue repair, and the resolution of inflammation. These interactions provide dynamic regulatory mechanisms in various pathological conditions and have potential implications for therapeutic intervention.

The current results indicate that chemotherapy regimens for SCC can exert immunostimulatory effects on various SCC cell lines. In particular, treatment with DDP, NDP, OXA, and DOC significantly increased the release of DAMPs *in vitro*. These findings are consistent with the results of our *in vivo* vaccination assay, which showed that mice treated with chemotherapeutic agents had a 100% tumor-free survival rate. Therefore, further investigation into the potential for DAMPs to increase the efficacy of chemotherapy is warranted.

The present study used Chinese tumor models to investigate the immunogenic potential of the second-generation platinum drugs CBP and NDP, the third-generation platinum drug LBP, and the first-generation drug DDP. CBP has not been extensively studied and its immunostimulatory effect is unclear from the available data. Although some studies have shown that CBP failed to induce immunomodulatory molecules in an MC38 hormonal mouse model [27], it was shown to effectively induce DAMPs and promote ICD development in breast cancer models [28]. However, in Chinese tumor models the effect of CBP on the release of DAMPs is very different to that of other platinum-based drugs that induce ICD. NDP and LBP are independently developed platinum drugs in China that are commonly used in clinical treatment. Although the induction of ICD by NDP and LBP has not been extensively studied, our *in vitro* experiments using different models (cervical SCC and esophageal SCC cell lines) confirmed their ability to induce ICD. Although our *in vitro* experiments showed that both NDP and LBP have good DAMP induction potential, our *in vivo* experiments found that LBP was not as effective as NDP. Similar to previous studies, OXA was found here to induce ICD. The present study also found that both DDP and CBP have ICD-inducing effects. However, DDP did not appear to activate the downstream PRR that subsequently induces immune maturation through CRT or HMGB1. The key molecules involved in this process remain to be identified and will be explored further in subsequent experiments.

It is well-known that platinum-derived chemotherapy drugs induce cytotoxicity by forming inter- or intra-strand DNA adducts [29]. As an inducer of ICD, OXA has been shown to induce endoplasmic reticulum stress and to promote early- to mid-stage cytosolic expression of CRT, as well as late-stage extracellular release of HMGB1 [30,31]. In contrast to OXA, DDP does not activate protein kinase-like ER kinase (PERK)-dependent phosphorylation of eukaryotic translation initiation factor 2α (eIF2 α). Consequently, there is no formation of stress granules or autophagy, which occur only after eIF2 α phosphorylation [32]. Although DDP is not usually considered to be an effective inducer of ICD, our animal model of cervical SCC showed that it could induce ICD. The effect of platinum drugs on the release of DAMPs may therefore vary between cancer types. Moreover, the complexity of the tumor microenvironment should also be considered when studying key molecules involved in the induction of ICD. There is currently a paucity of research on the second-generation platinum drug CBP, and it is still unclear whether it induces ICD. Differences between CBP and other platinum-based drugs in relation to their effects on the expression of immunomodulatory molecules have been observed in mouse models. CBP has been shown to effectively induce DAMPs in breast cancer models. Although NDP and LBP are common platinum drugs used in clinical treatment in China, their ability to induce ICD has not been extensively studied. Our *in vitro* experiments found that both NDP and LBP significantly induce DAMPs. However, our *in vivo* experiments showed that LBP was less effective than NDP. DDP and CBP also showed ICD-inducing effects in our study, but further research is needed to better understand the underlying mechanisms. Overall, our findings suggest that additional investigations are warranted into the ICD-inducing effects of platinum drugs in different cancer types.

TAX stabilizes microtubules by acting on the microtubule protein system, leading to mitotic cell death and blocking of the G2-M cell cycle [29]. TAX is considered to be an effective inducer of ICD based on research using mouse breast (4T1), colorectal (CT26 and MC38), lung (LL/2), and ovarian (ID8 and ID8F3) cancer cell lines, as well as human colorectal cancer cells (HCT116). TAX causes surface exposure of CRT and ERp57 in these tumor cells, accompanied by the extracellular release of ATP and HMGB1 [33]. Interestingly, our experiments also showed that TAX can induce the expression of HMGB1, ANXA1, HSP70, and certain levels of CRT. However, *in vivo* experiments showed that TAX does not function as an inducer of ICD, at least in SCC. Various indicators suggest that DAMPs are important adjuvant components in the ICD process, but do not fully indicate the occurrence of ICD. In conclusion, the role of DAMPs in ICD requires further exploration [7]. The physical form in which TAX is used also plays a significant role in its induction of ICD, with most studies reporting that TAX liposomes and nanoparticles

have a stronger induction effect on DAMPs. Various results also indicate that pure TAX does not effectively induce ICD [34]. Although research on DOC-induced DAMPs is limited, a study in non-small cell lung cancer revealed that DOC significantly increased the release of HMGB1, and this was associated with improved patient prognosis [35]. Additionally, DOC was shown to induce the exposure of CRT at the surface of breast, prostate and colorectal cancer cells [36]. In the present study, TAX significantly induced the release of DAMPs *in vitro*, but these effects were not replicated in the animal model. Moreover, we found that large quantities of DAMPs released at the cellular level did not circulate in the bloodstream. IHC analysis also revealed low expression levels of CRT and HMGB1 in the tumor-forming tissue at the site of reinoculation.

Our experimental approach was to evaluate the strength of induction of DAMP molecules by platinum drugs and TAX at the cellular level. To obtain accurate results, a multiplicative concentration treatment method was employed to determine the optimal action time and concentration threshold for each DAMP molecule. These results informed the subsequent animal experiments, which were conducted in three phases to validate each model. The *in vivo* experiments revealed that for an ICD effect to occur, sufficient amounts of DAMPs must be produced at the cellular level and must also reach a certain level in the tumor microenvironment and even in the bloodstream. Although drugs such as LBP and TAX induced significant amounts of DAMPs at the cellular level, these failed to reach the required levels in the bloodstream to induce ICD effects. Similarly, it is known that OXA and DOC not only kill tumor cells but also activate the immunogenic microenvironment, thereby accelerating tumor cell death. While CBP and DOC were found to induce ICD in our study, confirmation in a larger range of experimental models is needed. DDP is a non-inducer of ICD that nevertheless produced some ICD effects through a non-traditional mechanism. This also requires further study. NDP and LBP were developed in China and share similar structures and targets with other platinum drugs. However, LBP did not effectively induce DAMPs at the *in vivo* level, rendering it inactive as an ICD-inducing agent. In contrast, NDP showed promising results and is quite encouraging in view of its current scope of usage.

The present study involved a preliminary screening and exploration of the ICD-inducing effects of drugs used in clinical TP protocols. However, the mechanisms that underlie these effects were not thoroughly investigated here. Instead, our experimental focus was on a few unique molecules with significant DAMP activity. This may have led to some bias in the results and may not fully explain the ICD-inducing effects of each drug. Despite this, our results suggest that reducing the dosage of drugs, or combining them with immunological drugs, may provide clinical benefits for patients.

Recent clinical trial data supports the notion of combining a chemotherapeutic regimen with immunotherapy in order to generate an effective anti-tumor immune response [37–39]. By gaining novel insights into the immunogenic properties of tumors, this could lead to more rationally designed combination strategies that improve the clinical outcome of SCC patients.

5. Conclusion

In conclusion, our study presents novel data on the immunostimulatory effects of clinically relevant chemotherapeutic regimens used in the treatment of SCC patients. Platinum-derived drugs and TAX are the core components of chemotherapy regimens based on the TP protocol. These induce a certain degree of adjuvant effects, such as the extracellular release of DAMPs. However, only DDP, carboplatin, NDP, OXA and DOC can be classified as inducers of ICD.

Abbreviations

ICIs, Immune Check Point Inhibitors; ICBs, Immune Checkpoint Blockers; RCD, Regulate Cell Death; ICD, Immunogenic Cell Death; SCC, Squamous Cancer Cell; CRT, Calreticulin; HMGB1, High Mobility Group Protein B1; HSP70, Heat Shock Protein 70; ATP, Adenosine Triphosphate; DC, Dendritic Cells; PRR, Pattern Recognition Receptors; OXA, Oxaliplatin; CPA, Cyclophosphamide; DDP, Cisplatin; CBP, Carboplatin; NDP, Nedaplatin; LBP, Lobaplatin; TAX, Paclitaxel; DOC, Docetaxel; CCK-8, Cell Counting Kit-8; DMEM, Dulbecco's modified eagle medium; IC50, Half Maximal Inhibitory Concentration; IHC, Immunohistochemistry; PERK, Protein Kinase-like ER Kinase; eIF2 α , Eukaryotic Translation Initiation Factor 2 α ; DAMP, damage-associated molecular pattern; amRF, amplitude-modulated radiofrequency; TNBC, Triple-negative breast cancer; JNK, c-Jun N-terminal kinase.

Availability of Data and Materials

Data are available on request from the corresponding author.

Author Contributions

ML and YX: designed the study. ZH, XJ and XD: executed the study. XD: collected clinical information. ZH, LB, XJ, and XD: performed the literature search and collected the data. ZH, XJ, XD, XY and LB: analyzed and visualized the data. ZH, XJ, XD and LB: drafted the manuscript. XY, YX and ML: revised the manuscript. All authors contributed to editorial changes in the manuscript. All authors read and approved the final manuscript. All authors have participated sufficiently in the work and agreed to be accountable for all aspects of the work.

Ethics Approval and Consent to Participate

This study was approved by the Ethics Committee of Daping Hospital. Animal Ethics Approval Number: AMUWEC20237410, Human Ethics Approval Number: 2023(278). Written informed consent was obtained from all participant.

Acknowledgment

The authors would like to thank all participants who took part in the survey.

Funding

This work supported by grants from the National Natural Science Foundation of China (No.81902671) & (No. 82002444).

Conflict of Interest

The authors declare no conflict of interest.

Supplementary Material

Supplementary material associated with this article can be found, in the online version, at <https://doi.org/10.31083/j.fbl2904158>.

References

- [1] Apetoh L, Ghiringhelli F, Tesniere A, Obeid M, Ortiz C, Criollo A, *et al.* Toll-like receptor 4-dependent contribution of the immune system to anticancer chemotherapy and radiotherapy. *Nature Medicine*. 2007; 13: 1050–1059.
- [2] Topalian SL, Hodi FS, Brahmer JR, Gettinger SN, Smith DC, McDermott DF, *et al.* Safety, activity, and immune correlates of anti-PD-1 antibody in cancer. *The New England Journal of Medicine*. 2012; 366: 2443–2454.
- [3] Green DR, Oguin TH, Martinez J. The clearance of dying cells: table for two. *Cell Death and Differentiation*. 2016; 23: 915–926.
- [4] Nagata S, Hanayama R, Kawane K. Autoimmunity and the clearance of dead cells. *Cell*. 2010; 140: 619–630.
- [5] Yatim N, Cullen S, Albert ML. Dying cells actively regulate adaptive immune responses. *Nature Reviews. Immunology*. 2017; 17: 262–275.
- [6] Aria H, Rezaei M. Immunogenic cell death inducer peptides: A new approach for cancer therapy, current status and future perspectives. *Biomedicine & Pharmacotherapy = Biomedecine & Pharmacotherapie*. 2023; 161: 114503.
- [7] Xie D, Wang Q, Wu G. Research progress in inducing immunogenic cell death of tumor cells. *Frontiers in Immunology*. 2022; 13: 1017400.
- [8] Liu X, Yao S, Feng Y, Li P, Li Y, Xia S. Construction of a Novel Damage-Associated Molecular-Pattern-Related Signature to Assess Lung Adenocarcinoma's Prognosis and Immune Landscape. *Biomolecules*. 2024; 14: 108.
- [9] Garg AD, More S, Rufo N, Mece O, Sassano ML, Agostinis P, *et al.* Trial watch: Immunogenic cell death induction by anticancer chemotherapeutics. *Oncoimmunology*. 2017; 6: e1386829.
- [10] Vanmeerbeek I, Sprooten J, De Ruyscher D, Tejpar S, Vandenberghe P, Fucikova J, *et al.* Trial watch: chemotherapy-induced immunogenic cell death in immuno-oncology. *Oncoimmunology*. 2020; 9: 1703449.
- [11] Jiang M, Zeng J, Zhao L, Zhang M, Ma J, Guan X, *et al.* Chemotherapeutic drug-induced immunogenic cell death for nanomedicine-based cancer chemo-immunotherapy. *Nanoscale*. 2021; 13: 17218–17235.
- [12] Sukkurwala AQ, Adjemian S, Senovilla L, Michaud M, Spaggiari S, Vacchelli E, *et al.* Screening of novel immunogenic cell death inducers within the NCI Mechanistic Diversity Set. *Oncoimmunology*. 2014; 3: e28473.
- [13] Galluzzi L, Vitale I, Warren S, Adjemian S, Agostinis P, Martinez AB, *et al.* Consensus guidelines for the definition, detection and interpretation of immunogenic cell death. *Journal for Immunotherapy of Cancer*. 2020; 8: e000337.
- [14] Gu Z, Hao Y, Schomann T, Ossendorp F, Ten Dijke P, Cruz LJ. Enhancing anti-tumor immunity through liposomal oxaliplatin and localized immunotherapy via STING activation. *Journal of Controlled Release: Official Journal of the Controlled Release Society*. 2023; 357: 531–544.
- [15] Limagne E, Thibaudin M, Nuttin L, Spill A, Derangère V, Fumet JD, *et al.* Trifluridine/Tipiracil plus Oxaliplatin Improves PD-1 Blockade in Colorectal Cancer by Inducing Immunogenic Cell Death and Depleting Macrophages. *Cancer Immunology Research*. 2019; 7: 1958–1969.
- [16] Rodrigues MC, Morais JAV, Ganassin R, Oliveira GRT, Costa FC, Morais AAC, *et al.* An Overview on Immunogenic Cell Death in Cancer Biology and Therapy. *Pharmaceutics*. 2022; 14: 1564.
- [17] Tsutsumi H, Inoue H, Shiraishi Y, Hirayama A, Nakanishi T, Ando H, *et al.* Impact of increased plasma levels of calreticulin on prognosis of patients with advanced lung cancer undergoing combination treatment of chemotherapy and immune checkpoint inhibitors. *Lung Cancer (Amsterdam, Netherlands)*. 2023; 181: 107264.
- [18] Zhang Y, Akhil V, Seo HS, Park HR, Kim SH, You SH, *et al.* The combination of calreticulin-targeting L-ASNase and anti-PD-L1 antibody modulates the tumor immune microenvironment to synergistically enhance the antitumor efficacy of radiotherapy. *Theranostics*. 2024; 14: 1195–1211.
- [19] Tang D, Kang R, Berghe TV, Vandenabeele P, Kroemer G. The molecular machinery of regulated cell death. *Cell Research*. 2019; 29: 347–364.
- [20] Amiri M, Molavi O, Sabetkam S, Jafari S, Montazersaheb S. Stimulators of immunogenic cell death for cancer therapy: focusing on natural compounds. *Cancer Cell International*. 2023; 23: 200.
- [21] Elliott MR, Chekeni FB, Trampont PC, Lazarowski ER, Kadl A, Walk SF, *et al.* Nucleotides released by apoptotic cells act as a find-me signal to promote phagocytic clearance. *Nature*. 2009; 461: 282–286.
- [22] Troitskaya OS, Novak DD, Richter VA, Koval OA. Immunogenic Cell Death in Cancer Therapy. *Acta Naturae*. 2022; 14: 40–53.
- [23] Li C, Wang X, Chen T, Li W, Zhou X, Wang L, *et al.* Huaier Induces Immunogenic Cell Death *Via* CircCLASP1/PKR/eIF2 α Signaling Pathway in Triple Negative Breast Cancer. *Frontiers in Cell and Developmental Biology*. 2022; 10: 913824.
- [24] Sverchinsky DV, Alhasan BA, Mikeladze MA, Lazarev VF, Kuznetcova LS, Morshneva AV, *et al.* Autocrine regulation of tumor cell repopulation by Hsp70-HMGB1 alarmin complex. *Journal of Experimental & Clinical Cancer Research: CR*. 2023; 42: 279.
- [25] Minnaar CA, Szasz A. Forcing the Antitumor Effects of HSPs Using a Modulated Electric Field. *Cells*. 2022; 11: 1838.
- [26] Nair S, Arora S, Lim JY, Lee LH, Lim LHK. The regulation of TNF α production after heat and endotoxin stimulation is dependent on Annexin-A1 and HSP70. *Cell Stress & Chaperones*. 2015; 20: 583–593.
- [27] Schaer DA, Geeganage S, Amaladas N, Lu ZH, Rasmussen

- ER, Sonyi A, *et al.* The Folate Pathway Inhibitor Pemetrexed Pleiotropically Enhances Effects of Cancer Immunotherapy. *Clinical Cancer Research: an Official Journal of the American Association for Cancer Research*. 2019; 25: 7175–7188.
- [28] Golden EB, Frances D, Pellicciotta I, Demaria S, Helen Barcellos-Hoff M, Formenti SC. Radiation fosters dose-dependent and chemotherapy-induced immunogenic cell death. *Oncoimmunology*. 2014; 3: e28518.
- [29] Gallego-Jara J, Lozano-Terol G, Sola-Martínez RA, Cánovas-Díaz M, de Diego Puente T. A Compressive Review about Taxol[®]: History and Future Challenges. *Molecules (Basel, Switzerland)*. 2020; 25: 5986.
- [30] Wang J, Zhang H, Yin X, Bian Y. Oxaliplatin Induces Immunogenic Cell Death in Human and Murine Laryngeal Cancer. *Journal of Oncology*. 2022; 2022: 3760766.
- [31] Zhu H, Shan Y, Ge K, Lu J, Kong W, Jia C. Oxaliplatin induces immunogenic cell death in hepatocellular carcinoma cells and synergizes with immune checkpoint blockade therapy. *Cellular Oncology (Dordrecht)*. 2020; 43: 1203–1214.
- [32] Martins I, Kepp O, Schlemmer F, Adjemian S, Tailler M, Shen S, *et al.* Restoration of the immunogenicity of cisplatin-induced cancer cell death by endoplasmic reticulum stress. *Oncogene*. 2011; 30: 1147–1158.
- [33] Lau TS, Chan LKY, Man GCW, Wong CH, Lee JHS, Yim SF, *et al.* Paclitaxel induces immunogenic cell death in ovarian cancer via tlr4/ikk2/snare-dependent exocytosis. *Cancer Immunology Research*. 2020; 8: 1099–1111.
- [34] Zhai J, Gu X, Liu Y, Hu Y, Jiang Y, Zhang Z. Chemotherapeutic and targeted drugs-induced immunogenic cell death in cancer models and antitumor therapy: An update review. *Frontiers in Pharmacology*. 2023; 14: 1152934.
- [35] Gao Q, Wang S, Chen X, Cheng S, Zhang Z, Li F, *et al.* Cancer-cell-secreted CXCL11 promoted CD8⁺ T cells infiltration through docetaxel-induced-release of HMGB1 in NSCLC. *Journal for Immunotherapy of Cancer*. 2019; 7: 42.
- [36] Hodge JW, Garnett CT, Farsaci B, Palena C, Tsang KY, Ferrone S, *et al.* Chemotherapy-induced immunogenic modulation of tumor cells enhances killing by cytotoxic T lymphocytes and is distinct from immunogenic cell death. *International Journal of Cancer*. 2013; 133: 624–636.
- [37] Gandhi L, Rodríguez-Abreu D, Gadgeel S, Esteban E, Felip E, De Angelis F, *et al.* Pembrolizumab plus Chemotherapy in Metastatic Non-Small-Cell Lung Cancer. *The New England Journal of Medicine*. 2018; 378: 2078–2092.
- [38] Novello S, Kowalski DM, Luft A, Gümüş M, Vicente D, Mazières J, *et al.* Pembrolizumab Plus Chemotherapy in Squamous Non-Small-Cell Lung Cancer: 5-Year Update of the Phase III KEYNOTE-407 Study. *Journal of Clinical Oncology: Official Journal of the American Society of Clinical Oncology*. 2023; 41: 1999–2006.
- [39] Paz-Ares L, Luft A, Vicente D, Tafreshi A, Gümüş M, Mazières J, *et al.* Pembrolizumab plus Chemotherapy for Squamous Non-Small-Cell Lung Cancer. *The New England Journal of Medicine*. 2018; 379: 2040–2051.